

The Effects of Snow Cover on the Dynamic Pressure of Nuclear Detonation Blast Waves

By: Capt. Adam Card and Lt. Col. Andrew Decker

Introduction

Blast pressure is the primary military targeting metric for nuclear weapons. Any local conditions that affect blast pressure have the potential for altering nuclear plans, both from defensive and offensive standpoints. Understanding the impact of snow to the blast wave, therefore, provides a benefit both to military planners and to warfighters on the ground, for any operation occurring in arctic environments.

No existing data provides a quantitative description of how snow on the ground affects a nuclear detonation blast wave passing over it. Similar blast waves passing over dust have experimentally proven to enhance blast pressure in a localized region.¹ This research seeks to understand the snow lofting mechanism and determine quantitative results to dynamic and total pressures within the blast wave.

The research strategy selected to investigate this topic included conducting several scale experiments using a shock tube. Shock waves, once produced, are very similar regardless of source. If a lab-created shock front transited over snow or a snow-proxy, researchers could determine the pressure delta by comparing those measurements against similar data recorded from a shock front passing over an ideal surface. This result could then improve the understanding of how shock waves created by detonations behave in larger correlating environments.

Theory

OVERPRESSURE

Shock forms when an area of high pressure develops in a short period of time, as in the case of an explosive detonation. In an attempt to reach equilibrium, the pressure moves by means of a discontinuous wave into the surrounding environment, generally taking the form of the relationship shown in Figure 1. Nuclear literature refers to the delta above ambient pressure as “overpressure” and the delta below ambient as “negative pressure.”

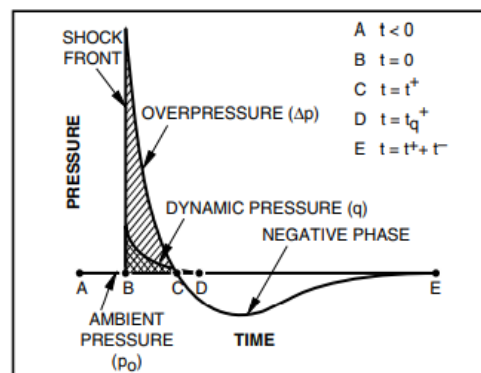


FIGURE 1: Pressure-time relationship for an ideal blast wave.²

As shown in Figure 1, shock waves consist of an initial overpressure wave followed by a negative pressure wave of lesser magnitude, both of

which can be damaging to targets. The peak pressure of the shock wave deteriorates with time and distance from the initiation point as the high-density gases spread out; this static pressure relationship takes the form shown in Equation 1,³

EQUATION 1:
$$p_1 = p_{ref} \frac{r_{ref}^3}{r^3}$$

where p_2 is the shock front pressure at the time of interest, r is the distance from ground zero at that time, p_{ref} is the reference pressure at some early time after detonation, and r_{ref} is the correlating shock front distance from ground zero at that early time. As pressure deteriorates, the velocity of the shock wave decreases, causing the duration of the pressure pulse to increase with distance from ground zero.

The phenomena discussed up to this point have been components of static pressure, which is due to the force caused by the random molecular motion in a fluid. There is also a second component to total pressure: dynamic pressure. Dynamic pressure is a force caused by the directional movement of a fluid – and thus contains a vector component. In a shock wave, it constitutes the movement of mass in the medium the wave passes through. This fluid movement, or “wind gust,” can be thought of as the kinetic energy of the shock front. Together, these two components sum to produce total pressure as seen in Equation 2,⁴

EQUATION 2:
$$p_{total} = p_{static} + p_{dynamic}$$

where p_{total} , p_{static} , and $p_{dynamic}$ represent their respective pressure components.

At equilibrium, a static pressure may exist without dynamic pressure. As a region of localized static overpressure occurs, however, the gas begins to accelerate away from the area of higher static pressure towards areas of lower static pressure. This movement creates an increase in directional force and, thus, dynamic pressure. The relationship in an ideal gas, which also holds true for a nuclear detonation over an ideal surface, can be described by Equation 3,⁵

EQUATION 3:
$$q = \frac{5\Delta p^2}{2(7p_0 + \Delta p)}$$

where q is the peak dynamic pressure, Δp is the peak overpressure, and p_0 is the atmospheric pressure. The graphical representation is shown in Figure 2. This relationship does not hold over non-ideal surfaces.⁶

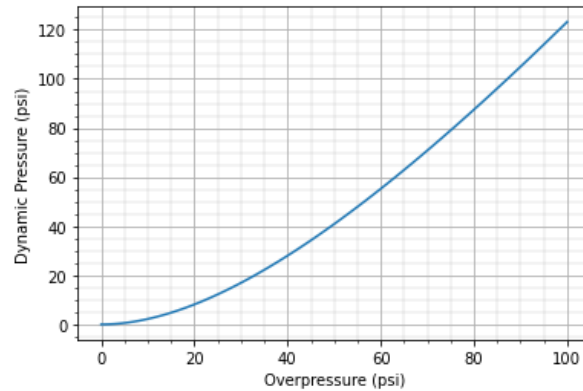


FIGURE 2: The relationship of dynamic pressure to static overpressure in an ideal gas for a burst on an ideal surface.

PRECURSOR WAVES

Thermally non-ideal surfaces (e.g. desert sand, coral, asphalt, etc) absorb substantial amounts of heat due to the thermal pulse resulting from a nuclear detonation. This process creates a layer of hot air near the ground containing dust, dirt, and other particulate matter that forms prior to the arrival of the blast wave. For appropriate heights-of-burst, this thermal layer creates a region where the blast wave may propagate faster than the primary wave. Energy losses from upward pressure expansion in this precursor wave prevent it from continuously outrunning the shock front; once formed, it constitutes a static feature ahead of the blast wave. The particulate matter entrained in the precursor has the possibility of increasing dynamic pressures while simultaneously decreasing static overpressures.⁷ A graphic of a precursor wave can be seen in Figure 3.

LITERATURE REVIEW

Some prior experimentation as far back as the 1960s used conventional explosives over snowy surfaces. These tests produced decreased static overpressure effects at a given radius;⁹ snow cover appears to effectively “dampen” explosive blast waves. The major driver of this “dampening” effect is the non-ideal nature of the surface; explosive energy is transmitted into the snow to crush, loft, or move it. Consequently, less energy is available for reflection and contribution to the outward-moving shock front, resulting in lower static overpressure. Snow depth and density did not have notable effects on static pressure, however.

Multiple sources indicated potentially different effects for the dynamic pressure component.¹⁰ These sources noted that snow should behave similarly to dust, which initially consumes energy (as reflected by decreased static overpressures) to loft and accelerate, but then provides the blast wave with additional mass and momentum, leading to increased dynamic and total pressures. Quantitative data validated this effect over desert and grasslands,¹¹ but subsequent research provided no further verification to confirm snow's similar behavior. Of particular note, both sources indicated that a blast precursor played some catalyzing role in lofting the material to allow greater entrainment.

Because it is unclear whether light snow of the type used in this study is classified as a thermally ideal or non-ideal material, it was indeterminable whether a blast precursor would form over snow as over dust. Consequently, this research assumed no precursor.

Method

This study included three sets of tests, labeled A, B, and C. Test set A measured peak total pressures, test set B measured total pressure impulse, and test set C recorded static and (subsequently calculated) dynamic pressure impulses. Each set of tests included two subsets: one for ideal surfaces, conducted in a clean shock tube, and a second for non-ideal surfaces, which involved the deposition of one inch of surrogate snow on the floor of the shock tube prior to detonation (described in greater detail below).

The shock tube used in both tests was a horizontally-oriented explosive-powered device, eight feet long with a rectangular 1x12-inch cross-section, as shown in Figure 4. An ethylene-oxygen fuel mix was ignited and driven to supersonic speed. This blast propagated down the length of the tube. The end, unsealed, allowed gases to escape. Piezoelectric sensors, which use crystal-lattice deformation of certain materials to provide an electrical measurement of force,¹² measured pressure at various displacements from the initiation point. Researchers placed sensors both within the fluid flow (measuring total pressure) and orthogonal to flow on the walls (measuring static pressure).

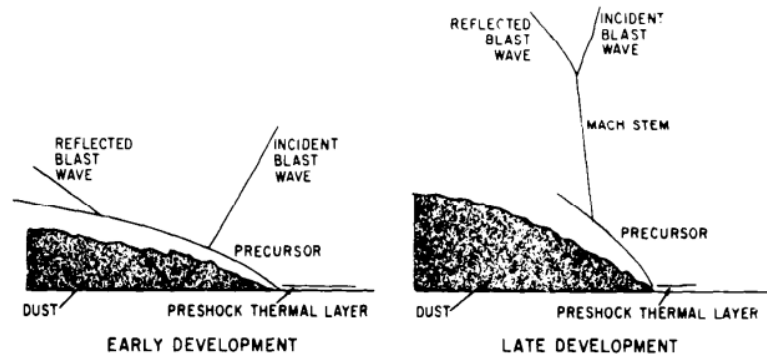


FIGURE 3: Development of the precursor wave.⁸



FIGURE 4: Shock tube, displaying to the right the shock wave generation apparatus that propagates into the rectangular tube, left. Although currently clean for an ideal test, material piled on the floor allows for non-ideal tests.

The piezoelectric sensors were PCB 113B28s, suitable for pressure readings up to 50 psi. As only one sensor was initially available, the first test set involved only the measurement of total pressures. Sensor signals routed through a PCB 482 signal conditioner before reading out at a Tektronix MDO3024 Mixed Domain Oscilloscope. The voltage signals exported via .csv file to a computer, which converted the pressure readings and provided graphical outputs. Calibration sheets provided with the sensors indicated conversion factors of 113 and 101 mV/psi, respectively.

Initially, the non-ideal test medium was a polymer-based synthetic snow. The density of this material, as mixed, was between 0.26 and 0.34 g/cm³, consistent with snow densities found in literature.¹³ Initial test runs revealed that the adhesiveness of the synthetic snow was not representative of real snow and negatively impacted test legitimacy, necessitating a new medium. Damp sawdust, often used in the

snowblower industry as a proxy for snow during machine testing,¹⁴ was the subsequent snow proxy. The sawdust had a measured density of 0.26 g/cm³, which remained within the range of snow densities found in literature. All results reported in this study used the damp sawdust medium for non-ideal surface tests.

TEST SET A: PEAK TOTAL PRESSURES

Test Set A used one sensor for sequential measurements at 24 separate test positions. These positions were located in a matrix of horizontal and vertical coordinates. Horizontal coordinates consisted of 16, 36, 60, and 84 inches from the point of detonation, while vertical coordinates rose from the floor of the shock tube to 6 inches in height, in 1-inch increments. This arrangement created a subset of six sensor positions at each of the four horizontal distances, for a total of 24 positions. Physical limitations of the sensor fixture resulted in the base position being ¼ inch above the actual floor. At each vertical-horizontal position, five measurements provided a basis for uncertainty. For Test Set A, the single sensor affixed to the end of a stiff tube and oriented directly into the flow measured total pressure. This initial test examined the peak pressures over ideal and non-ideal surfaces.

TEST SET B: TOTAL PRESSURE IMPULSE

Test Set B used one sensor to examine pressure impulse: the total application of force over a period of time. The period of time chosen approximated the duration of the first positive pressure pulse, about 1 ms. For this test set, researchers examined only six sequential positions: those 16 inches from the point of detonation.

TEST SET C: STATIC AND DYNAMIC PRESSURE IMPULSES

Unlike the previous tests, Test Set C utilized two piezoelectric sensors run simultaneously. The second piezoelectric sensor mounted at the same position but orthogonal to the first sensor (and to the fluid flow), allowed for measurement of the static pressure impulse. The use of the first sensor to simultaneously take a total pressure impulse reading at the same point, as shown in Figure 5, allowed researchers to make subsequent calculations of dynamic pressure impulse. Due to mounting geometry limitations,

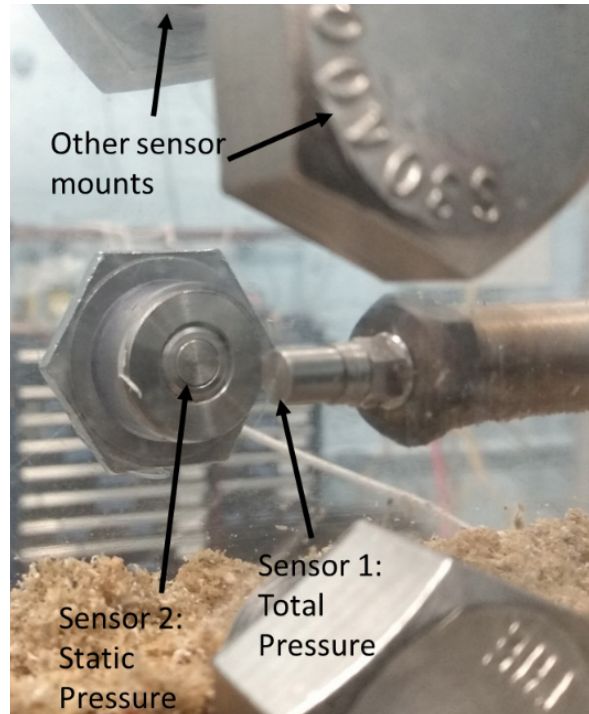


FIGURE 5: Test Set C mounting configuration. Sensor 1, mounted with an orientation towards the shock wave origin, measures total pressure impulse. Sensor 2, mounted orthogonal to the flow but at the same location, measures static pressure (overpressure) impulse. Other static pressure sensor mounting points are visible, but each test ran sequentially as a paired measurement of both sensors.

the minimum measurement height increased to 1 inch. Like the previous tests, researchers recorded five measurements at each point.

Results & Discussion

TEST SET A RESULTS

The results from the Test Set A, observation of peak pressures, are shown in Figure 6. Error bars are derived from the standard deviation of the five samples taken at each test point. A clear trend is observable for the ideal shocks as distance increases from initiation. While pressures near the floor are depressed early on, they catch and then exceed pressures far from the floor. This phenomenon is not well understood, but may be due to complications from the multi-point shock feeding mechanism. Non-ideal tests reveal that shocks over the dry sawdust mimic the ideal shocks far from the floor, but proximity to the non-ideal surface results in correlatingly depressed pressures. This effect indicates that

the non-ideal surface has a regional effect; far from its influence the shock wave returns to ideal behavior.

TEST SET B RESULTS

The results from Test Set B, observation of pressure impulses, are shown in Figure 7. The non-ideal surface demonstrates a negative impact on the total pressure impulse magnitudes. However, in the area near but not at the floor, an area of increased magnitude for the non-ideal test is observable before tapering off with distance from the non-ideal surface. It is possible that this phenomenon is a repetition of the non-ideal blast behavior demonstrated in past work, where increased dynamic pressure is obtained at the cost of decreased static pressure. If this is the case, however, the static pressure cost is too high to benefit the overall total pressure impulse.

TEST SET C RESULTS

The results from the third iteration of testing, observation of static and total pressure impulses, along with the calculation of associated dynamic pressure impulses, are shown in Figure 8. Similar to findings in the total pressure case, a mild effect is observable in the region near the non-ideal surface. Static pressure is depressed as energy is used to loft and accelerate the damp sawdust particles, but those particles provide additional momentum to the shock front in the near-floor region, enhancing dynamic pressure impulses.

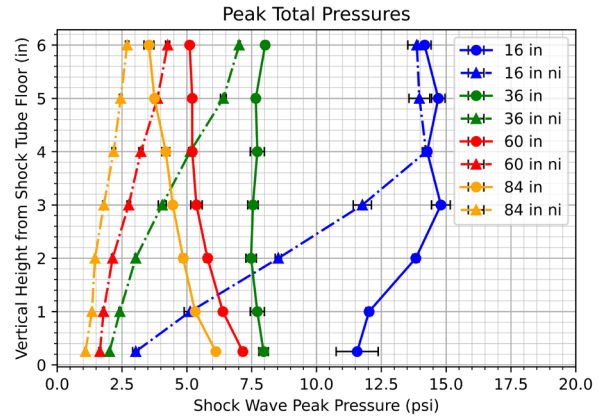


FIGURE 6: Peak total pressures. Non-ideal behavior occurs only near the floor, in the region of the non-ideal surface.

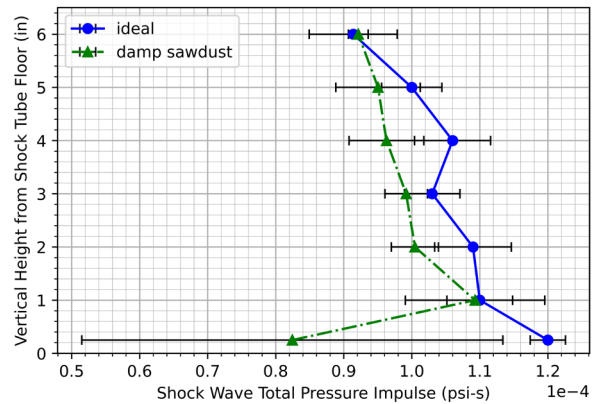


FIGURE 7: Total pressure impulses. The non-ideal surface generally depresses the total pressure impulse magnitude.

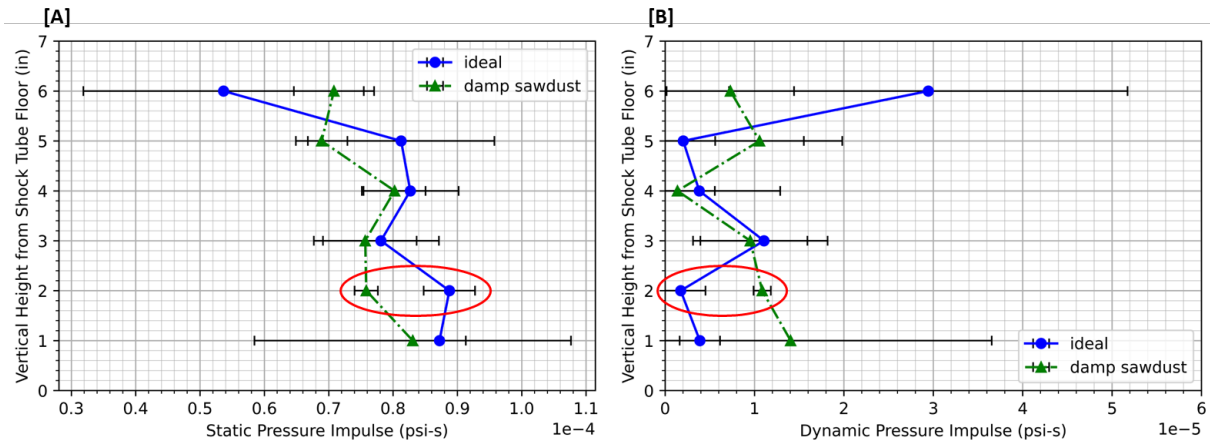


FIGURE 8: [A] Static pressure impulse variation. [B] Dynamic pressure impulse variation. Correlating areas of interest are highlighted in each subplot; for a localized area, as static pressure impulse decreases in the non-ideal case, dynamic pressure impulse increases. Note that the x-axes on these plots are *not* equivalent, to allow for detailed analysis of the dynamic pressure impulses.

Observation of Figure 9, however, is sufficient to demonstrate that gains made by the dynamic pressure impulse are generally insufficient to offset the losses taken by the static pressure impulse. While a weak exception is noticeable near the floor, it is unclear if this point is distinct from uncertainty.

Conclusion

This research focused on quantifying the impact of ground-blanketing snowfall on nuclear detonation blast effects. Generally, it appears that an increase in dynamic pressure is possible in localized areas above the non-ideal snow proxy. If this is the case, however, those instances are not sufficient to overcome the static pressure reduction cost, resulting in equivalent or reduced total pressure. The experiments conducted indicated that although dynamic pressure impulses increase in magnitude by up to 250% over a snow proxy, corresponding overpressure decreases by as much as 15%, and the greater dependence of total pressure upon the overpressure value results in decreased overall pressures.

Prior experiments that demonstrated increased blast pressures over dust exhibited blast precursors. These precursors created jets of air ahead of the blast wave that lofted ground material into the path of the oncoming shock, allowing ready entrainment. It appears that without such a precursor, entrainment is minimal.

For operational troops, this research implies no adverse impact to operating in a snowy environment with regards to nuclear blast effects. That implication is likely to hold unless local conditions lead to substantial sustained air entrainment of snow, as might be the case in an Antarctic environment, where high winds may blow for hours or days.¹⁵ However, further research would be needed to confirm the veracity of such environmental impacts.

FUTURE WORK

Due to time and resource constraints, this research included only five repetitions at a limited number of locations. Future work might examine additional repetitions, and potentially more shock tube locations, to verify the regional effects seen near non-ideal surfaces in this work.

The development of a high-fidelity physics model with the aim of understanding the probability of

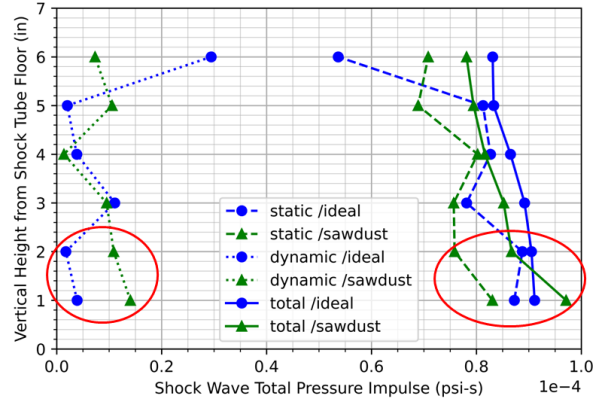


FIGURE 9: All impulse pressure components (error bars omitted to reduce clutter). Only near the floor is there any indication that dynamic pressure improvements may lead to increased total pressure. Large error bars (seen by pressure component in Fig. 8) make it difficult to draw meaningful conclusions from these results.

a precursor over snow would be the logical next step for this research. Validation of precursor existence would naturally lead to additional testing with precursor-simulated effects. ■

Capt. Adam Card

is a US Air Force officer and a doctoral candidate at the Air Force Institute of Technology. He holds a B.S.E. in Mechanical Engineering from Calvin University and an M.S. in Nuclear Engineering from the Air Force Institute of Technology. His email address is adam.card.1@us.af.mil.

Lt. Col. Andrew Decker

is a US Army FA52 officer and the Director of the DTRA Nuclear Science and Engineering Research Center at West Point, NY. He is also an Adjunct Professor of Nuclear Engineering at the Air Force Institute of Technology (AFIT). LTC Decker holds a B.S. in Psychology from the United States Military Academy, an M.S. in Nuclear Engineering from AFIT, and a Ph.D. in Nuclear Engineering from the University of Tennessee, Knoxville. His email address is andrew.decker@westpoint.edu.

Notes

1. Ozer Ingra and Gabi Ben-Dor, "Dusty Shock Waves," *Applied Mechanics Reviews* 41, no. 11 (November 1988): 379–437; O. Ingra, X. Wu, G. Q. Hu, and J. Falcovitz, "Shock Wave Propagation into a Dust-Gas Suspension Inside a Double-Bend Conduit," *Journal of Fluids Engineering* 124 (June 2002): 483–91; Noel H. Ethridge et al., *Real Surface (Non-Ideal) Effects on Nuclear Explosion Airblast from PRISCILLA-type Events*, (Aberdeen, MD: Applied Research Associates Inc., 1995).
2. John A. Northrop and Donald C. Sachs, *Capabilities of Nuclear Weapons: Effects Manual One*, (Alexandria, VA: Defense Nuclear Agency, 1994).
3. George F. Kinney, and Kenneth J. Graham, *Explosive Shocks in Air*, (New York: Springer, 1985).
4. Yunus A. Çengel, John M. Cimbala, and Robert H. Turner, *Fundamentals of Thermal-Fluid Sciences*, 4th ed. (New York: McGraw Hill, 2012).
5. Charles Bridgeman, *Introduction to the Physics of Nuclear Weapons*, (Fort Belvoir, VA: Defense Threat Reduction Agency, 2001).
6. Bridgeman, *Physics of Nuclear Weapons*.
7. Samuel Glasstone, and Philip J. Dolan, *The Effects of Nuclear Weapons*. 3rd ed. (Washington, D.C.: Department of Defense, 1994).
8. Glasstone and Dolan, *The Effects of Nuclear Weapons*.
9. Malcolm Mellor, *Cold Regions Science and Engineering Part III, Section A3A – Explosions and Snow*, (Hanover, NH: U.S. Army Cold Regions Research and Engineering Laboratory, 1965); L. F. Ingram, *Air Blast in an Arctic Environment*, (Vicksburg, MS: U.S. Army Engineer Waterways Experiment Station, 1962); J. Wisotski and W. H. Snyder, *A Study of the Effects of Snow Cover on High Explosive Blast Parameters*, (Denver: Denver Research Institute, 1966).
10. Northrop and Sachs, *Effects Manual One*; J.R. Keith and W. E. Wallace, *Handbook for Nuclear Weapons Effects under Arctic Conditions*, (Colorado Springs: Kama Sciences Corporation, 1980).
11. Fred M. Sauer, *Nuclear Airblast Precursor Dynamic Pressures Related to Surface Parameters*, (San Leandro, CA: Physics International Company, 1980); Ethridge et al., *PRISCILLA-type Events*.
12. C. Fleischer, "How Piezoelectricity Works," Autodesk, accessed September 22, 2022, <https://www.autodesk.com/products/eagle/blog/piezoelectricity/>.
13. Mellor, *Explosions and Snow*; Ingram, *Air Blast in an Arctic Environment*; H. Napadensky, *Dynamic Response of Snow to High Rates of Loading*, (Hanover, NH: U.S. Army Material Command Cold Regions Research and Engineering Laboratory, 1964).
14. Denis Aleshkov et al., "Experimental Investigations of Snow Bank Formation during Milling and Rotary Snow Blower Operation," *Journal of Applied Engineering Science* 19, no. 7 (January 2021).
15. Yuji Kodama, Gerd Wendler, and Joan Gosink, *The Effect of Blowing Snow on Katabatic Winds in Antarctica*, (Cambridge: Cambridge University Press, 2017).